JPP Journal of Pharmacy and Pharmacology

JPP 2001, 53: 999–1005

Received August 23, 2000
Accepted March 9, 2001
ISSN 0022-3573

Biostability and pharmacokinetics of LJP 920, an octameric Gal (α1–3) Gal conjugate for the inhibition of xenotransplantation rejection

Lee Jia, Matthew D. Linnik, Richard M. Jack and Lin Yu

Abstract

Antibodies to an α-galactosyl saccharide structure present in human serum are associated with hyperacute rejection and delayed xenograft rejection after pig-to-primate xenotransplantation. To overcome this major barrier to the xenotransplantation, LJP 920, a galactosyl α1–3 galactose (Gal (α1–3) Gal) coupled to a non-immunogenic platform at a valency of eight Gal (α1–3) Gal molecules/platform, was synthesized to clear circulating antibodies and to inhibit their production by B cells that produce these antibodies. Herein we report on the stability of LJP 920 in biological media and its pharmacokinetic profile. Incubation of LJP 920 with mouse serum or liver microsomes at 37°C for 2 days showed no indication of degradation of the conjugate as detected by a reversed-phase HPLC method, indicating that the conjugate is not subject to enzymatic metabolism. After intravenous administration of LJP 920 to mice at the doses of 20 and 100 mg kg^{-1}, LJP 920 serum concentration decreased rapidly, showing a biphasic pattern, with a distribution half-life of 3 min and an elimination half-life of more than 30 min, respectively. The serum-to-erythrocyte concentration ratio of LJP 920 was 33- and 36-fold excess at 0.5 and 5 min, respectively, after intravenous administration (100 mg kg^{-1}). Both C_{max} and AUC values increased in a dose-proportional manner. LJP 920 displayed a great distribution to well-perfused tissues. It was eliminated mainly through renal excretion in the unchanged form, which accounted for 23% of the total amount within 8 h of dosing.

Introduction

A shortage of human organs has driven research into the possibility of xenotransplantation using nonhuman donors (Bracy et al 1998; Nagasaka et al 1997). However, one barrier to xenotransplantation is hyperacute rejection and acute vascular rejection mediated by naturally occurring antibodies that are found in the serum of man. Unlike pigs and many mammalian species, the catarrhines (man, apes, and Old World monkeys) lack a functional α-1,3-galactosyltransferase (Larsen et al 1990; Galili & Swanson 1991; Joziasse et al 1991). Thus, they do not express the Gal (α1–3) Gal epitope. This, in turn, leads to the production of serum antibodies reactive with the Gal (α1–3) Gal epitope, most likely in response to exposure to Gal (α1–3) Gal-expressing native gut flora. (Galili et al 1987, 1993). These xenoreactive natural antibodies are thus available to bind to Gal (α1–3) Gal epitopes expressed on donor organs (Galili et al 1993; Sandrin et al 1993). This antibody binding is associated with hyperacute rejection, a combination of complement activation, platelet activation, thrombi formation in the graft vasculature and rapid death by necrosis of the ischaemic transplanted organ (Galili 1993).

La Jolla Pharmaceutical Company, 6455 Nancy Ridge Dr., San Diego, CA 92121, USA

Lee Jia, Matthew D. Linnik, Richard M. Jack, Lin Yu

Correspondence: L. Jia, Institute for Drug Development, 14960 Omicron Dr., San Antonio, TX 78245, USA.
E-mail: Ljia@saci.org

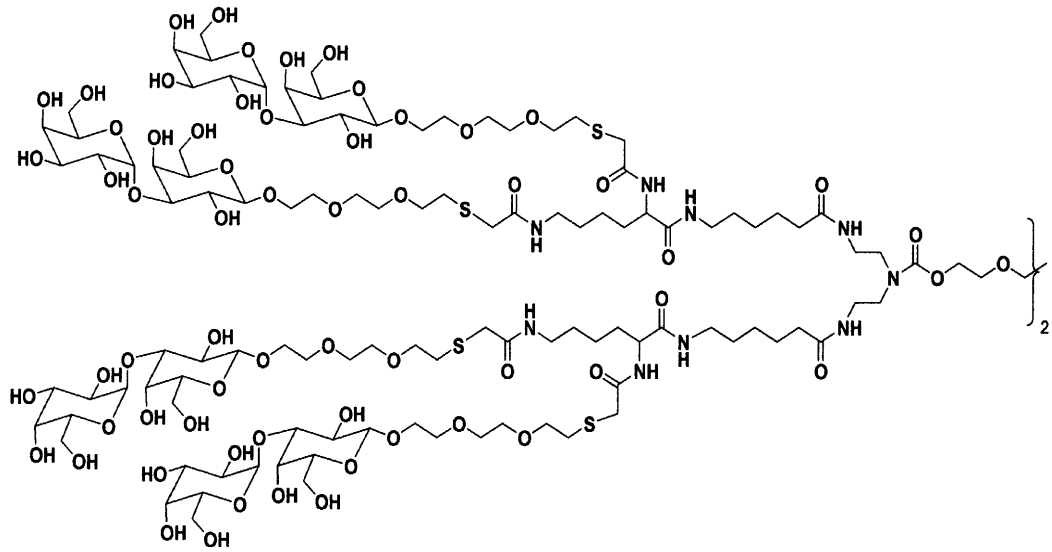

Figure 1 The structure of LJP 920.

For xenotransplantation to be successful, drugs must be developed to arrest the production by B lymphocytes of anti-α-galactose antibodies (tolerance) and clear the existing antibodies, and thus inhibit organ damage mediated by the antibodies.

We have recently synthesized a tolerogen designed to clear circulating α-galactose antibodies and inhibit antibody production by tolerizing the B cell population producing the pathogenic antibody. The synthesized tolerogen was composed of Gal (α1–3) Gal coupled to a non-immunogenic platform at a valency of eight Gal (α1–3) Gal molecules per platform to produce an octameric toleragen, LJP 920, with molecular weight 4261 (Figure 1), which is freely soluble in aqueous and organic solvents. In our laboratory studies, LJP 920 inhibited the binding of both human and nonhuman primate IgM and IgG pathogenic antibodies in-vitro. Furthermore, LJP 920 did not induce activation of complement, which promotes organ rejection in-vitro. LJP 920 treatment also showed a diminution in circulating IgG and IgM anti-Gal (α1–3) Gal antibodies during the course of an 8-day treatment in rhesus monkeys (Yu et al 1999).

A comprehensive knowledge of LJP 920 stability in biological media and its disposition in the body is critical for further development of the drug. If it is learned early that LJP 920 is not a substrate for the cytochrome P450 superfamily and serum enzymes, or that these enzymatic reactions represent only a minor contribution to overall metabolism of LJP 920, then concern is lessened for possible quick termination of the drug's activity. The pharmacokinetic parameters are equally important for a guide to the design of further investigation. Thus, the primary objective of this study was to determine the stability of the drug in serum and liver microsomes, and provide an assessment of its pharmacokinetic parameters in mice.

Materials and Methods

Preparation of mouse serum and liver microsomes

Balb/c mouse blood was collected from the ocular venous plexus by retro-orbital bleed. The serum was obtained after centrifugation of the blood at 5000 *g* for 10 min. Livers were quickly removed from ethically killed mice, and washed thoroughly with an ice-cold dilution buffer (potassium phosphate buffer (0.1 M, pH 7.4), 0.25 M sucrose and 0.1 mM EDTA). The livers were dissected and transferred to a 70-μm cell strainer (Becton Dickinson, Franklin Lakes, NJ) for washing with the dilution buffer to avoid blood contamination. The minced liver was homogenized with a motor-driven homogenizer in three volumes of the dilution buffer. The homogenate was then filtered through a 100-μm cell strainer to remove residual connective tissue. The filtrate was used to prepare liver microsomes by differential centrifugation at 4°C as described by Pearce et al (1996). Briefly, nuclei, mitochondria and lysosomes were removed by centrifugation at 10 000 *g* for 20 min, and the supernatant was spun using an ultracentrifuge model

Sorvall RC 70 (Kendro Lab Products, Newtown, CT) equipped with Oak Ridge polycarbonate tubes (Nalge Nunc International, Rochester, NY) at 105000 *g* for 60 min. The resulting supernatant fraction (cytosol) was stored at −80°C, and the pellet (microsomal fraction) was covered with the dilution buffer and removed from the underlying glycogen pellet with a vortex mixer. The microsomal pellet was then resuspended in the dilution buffer using a tissue grinder and centrifuged at 200000 *g* for 60 min. The microsomal pellet was resuspended in potassium phosphate buffer (pH 7.4, 10 mM), and the protein concentration of microsomes determined with a commercially available protein assay reagent (Bio-Rad, Hercules, CA). Bovine serum albumin served as standard. The microsomes were frozen at –80°C in 0.2-mL portions to minimize freeze–thaw cycles until use. The protein concentration of the working microsomal preparation was diluted to 2 mg mL^{-1} with the potassium phosphate buffer immediately before use.

Degradation reaction

One mL of serum or microsome solution containing 100 μg LJP 920 in a 1.5-mL Eppendorf tube was incubated at 37°C. The microsomal reaction was started by the addition of NADPH (1 mM). The initial time was recorded, and at known time intervals, 100 μL of reaction solution was removed and added to 200 μL of cold methanol to stop the enzymatic reactions and separate the target LJP 920 from the interfering serum and microsome components. The cloudy reaction solution was vortexed and then spun at 14 000 *g* for 15 min to pellet the precipitated proteins. The supernatant (50 μL) was analysed by HPLC to determine the residual concentrations of LJP 920 at various incubation times. The LJP 920 stability was also determined in precipitation supernatant containing methanol to ensure that the LJP 920 did not undergo methanol-catalysed degradation while awaiting HPLC sample analysis.

Dosing and sample collection

Balb/c mice of both sexes, 15–22 g, were purchased from Jackson Laboratory (Bar Harbor, ME). Dosing solutions of LJP 920 were prepared immediately before an experiment. The compound was diluted with phosphate buffered saline (10 mM, pH 7.4) to produce a final concentration of 2 and 10 mg mL^{-1}, respectively. The concentration of the solution was adjusted so that 200 μL administered to a 20-g mouse resulted in a dose of 20 or 100 mg kg^{-1}. The doses were administered intravenously via the lateral tail vein. Blood samples (250–300 μL) were collected by retro-orbital bleed at 0.5, 5, 10, 30, 60 and 120 min post-dose; three additional samples were collected from untreated mice and used as the blank. The serum and erythrocytes were separated by centrifugation at 5000 *g* for 10 min. After removal of the serum for HPLC assay, the buffy coat containing leucocytes and platelets was aspirated out with a pipette, and then the enriched erythrocytes were mixed with 2-fold excess of methanol by volume to lyse the erythrocytes. The methanol extracted LJP 920 from the erythrocytes. The mixture was then centrifuged at 14000 *g* for 10 min. The supernatant was used to directly detect the LJP 920 in erythrocytes.

For tissue distribution, the method was similar to that described previously (Jia et al 1999). Briefly, five mice were killed at 10 min and 2 h after intravenous administration of LJP 920 (100 mg kg^{-1}). Tissues were immediately removed and washed with 10 mM phosphate buffer. The tissues were then sliced and weighed. Blank or sample tissues ($\sim$ 0.5 g) were homogenized with 10 mM phosphate buffer (200 μL). Immediately after addition of methanol (200 μL) to the homogenate, the mixture was vortexed and centrifuged at 14000 *g* to obtain a clear supernatant, which was auto-injected (100 μL) into the HPLC column. For the excretion study, four mice receiving 100 mg kg^{-1} of LJP 920 (i.v.) were housed individually in metabolism cages (Nalge, Rochester, NY) for the cumulative collection of urine and faeces at 4 and 8 h after dosing. The pooled urine (100 μL) or faeces (0.1 g) were mixed with 200 μL methanol. The mixture was prepared for chromatographic analysis as described above.

Preparation of calibration standards

LJP 920 was synthesized by our chemical team. A working standard containing 5 mg mL^{-1} of LJP 920 was prepared in Milli Q H_2O. Seven calibration standards of LJP 920, 0.25–250 μg mL^{-1}, were prepared by supplementing blank pooled mouse sera with the diluted working standard. Serum (100 μL) spiked with a series of LJP 920 concentrations was added to 200 μL of methanol to precipitate serum proteins. The cloudy reaction sample was vortexed for 30 s and then spun at 14000 *g* for 15 min to pellet the precipitated proteins. A stock solution of 4-nitrophenyl-α-D-galactopyranoside (500 μg mL^{-1}) in Milli Q H_2O was added to the serum immediately before methanol precipitation at a final concentration of 125 μg mL^{-1} as an internal standard. Supernatant (100 μL) was auto-injected onto the HPLC. Sample recovery after precipitation of serum proteins with methanol was determined by comparison of the

peak area of LJP 920 and the internal standard at time zero with that of corresponding compounds of known concentrations in H_2O under the same treatments. The recovery of LJP 920 and the internal standard was $> 90\%$.

Analytical methods

Samples were analysed on a reversed-phase HPLC (Model HP 1100, Agilent, Palo Alto, CA) which consisted of an HP 1100 autosampler. The system was controlled and data were processed using ChemStation software. The HPLC analytical column (250×4.6 mm i.d.) was packed with 5-μm Intersil ODS-2 (MetaChem Inc., Torrance, CA) and maintained at 25°C in a column block heater. A guard column was employed to protect the analytical column. A mobile phase was composed of acetonitrile and H_2O (both HPLC grade). The gradient solution was 10–30% acetonitrile over 6 min, and then linear to 75% acetonitrile over 5 min at a flow rate of 1 mL min^{-1}. The sample was exclusively detected on peak area obtained for unchanged LJP 920 at a wavelength of 192 nm.

Data analysis

Serum LJP 920 concentrations in mice were back-calculated from the chromatographic standardization curve for LJP 920 in mouse serum. Pharmacokinetic parameters were calculated with the nonlinear least-square regression by using the computer program WinNonlin version 2.1 (Pharsight Co., Mountain View, CA). The serum concentration–time data of LJP 920 after intravenous administration were fitted to a bi-exponential model based on the goodness-of-fit criteria set by lower condition number, higher precision, lowest standard errors of the fitted parameters and the smallest value of Akaike Information Criterion (Gabrielsson & Weiner 1996), when comparing several models for a given set of data. The WinNonlin program uses the trapezoidal rule to calculate the area under the serum concentration–time curves (AUC) up to the last measured serum concentration. All other important parameters were analysed by the WinNonlin program.

Results and Discussion

Validation of assay performance

Under the present chromatographic conditions, the retention times for LJP 920 and its internal standard were 7.5 and 8.1 min, respectively (Figure 2). The octameric conjugate LJP 920 and its metabolites, disjointed Gal (α1–3) Gal moieties, could be clearly resolved under the chromatographic conditions. Peak areas increased linearly over the concentration range of LJP 920 (0.25–250 μg mL^{-1}) in both water and serum with correlation coefficients > 0.99. At the retention times, LJP 920 and its internal standard were eluted without any interfering peaks from the plasma (Figure 2), liver microsomes, tissue homogenates and urine. The biological matrix effects were determined using LJP 920 standards in water in comparison with those spiked in biological media, resulting in an overall chromatographic recovery of 92–109% that varied with LJP 920 concentrations. The result indicated a negligible matrix effect on the methanol extraction. The limit of quantitation was defined as the LJP920 concentration resulting in a peak area of 10 times of the noise level, and set at the lowest standard concentration on the calibration curve (0.25 μg mL^{-1}). To assess accuracy and precision, the inter-day imprecision (% coefficient of variation) and overall inaccuracy (% deviation from theoretical value)

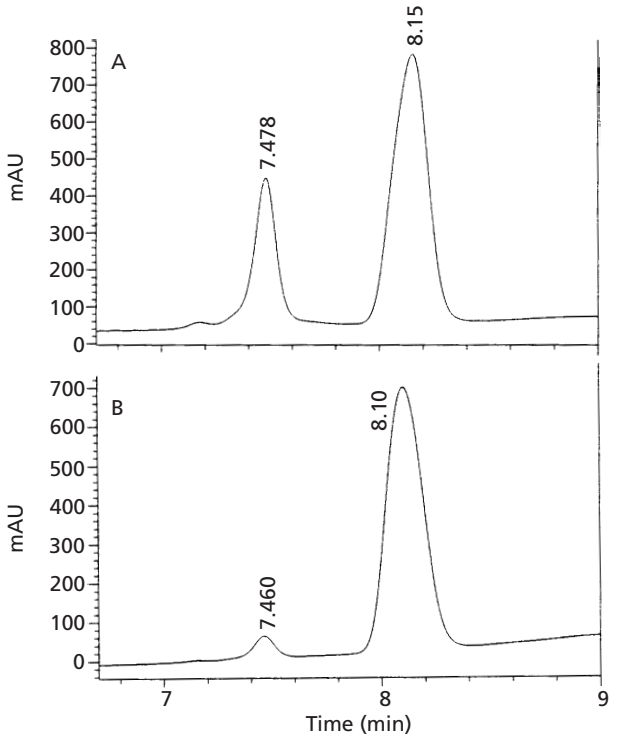

Figure 2 HPLC chromatograms obtained from the serum of mice administered with LJP 920 (20 mg kg^{-1}, i.v.). The chromatograms represent the concentration of LJP 920 in the serum withdrawn at 0.5 (A) and 5 min (B) after tail-vein injection. The retention times at 7.4 and 8.1 min correspond to LJP 920 and the internal standard, respectively.

were determined by replicate analysis (n = 6) of each LJP 920 concentration in serum over four separate analytical batches. Together with the intra-batch imprecision data from one of the analytical batches, the results of the method validation showed that the predicted concentrations of LJP 920 spiked in serum were within 10% of their theoretical values.

Biostability in serum and liver microsomes

The chromatographic peaks of authentic LJP 920 in biological media were identified by comparing the retention time of LJP 920 with that of the internal standard spiked in the same preparation in the presence and absence of the biological media. There was no significant degradation of LJP 920 when incubated with native serum or liver microsomes for 0.25, 0.5, 1, 2, 4, 8, 24 and 48 h (Figure 3). Extending the incubation of LJP 920 with serum for up to 100 h did not lead to any significant degradation. The observations indicate that LJP 920 is resistant to degradation in these biological media. In-vivo drug metabolism is reflected more reliably by in-vitro enzymatic catalysis by measuring the kinetics of degradation of drugs in-vitro (Birkett et al 1993; Obach et al 1997). The most mature technology for the in-vitro study of drug metabolism is associated with sera and liver microsomes, the latter containing the cytochrome P450 superfamily that biotransforms a variety of endogenous and exogenous compounds (Matsubara et al 1976). This in-vitro determination is one of the most important secondary screening assays in drug development, largely because it eliminates unstable candidate drugs and determines whether or not the in-vivo clearance is due to enzymatic degradation. Of greater interest in this study is the pronounced stability of LJP 920 in serum and liver microsomes (Figure 3). Using the same system, we found fast kinetics of degradation when insulin was incubated with serum and liver microsomes, indicating the kinetic activity of serum and microsomal enzymes in these studies. It is well known that drug elimination occurs by two major mechanisms, renal excretion and hepatic metabolism. Since LJP 920 is stable when incubated with serum or liver microsomes, concern is greatly reduced that the primary metabolism occurs in the liver.

Pharmacokinetic analyses

Serum levels of the two doses of LJP 920 declined in a similar fashion (Figure 4). The rapid decline of serum concentration of LJP 920 can be attributed to the distribution of LJP 920 from the central compartment to the peripheral compartment and renal excretion. There was a high consistency between observed and predicted concentrations and well-defined parameters with high precision when we simulated the LJP 920 pharmacokinetic profiles as a two-compartment open model. The pharmacokinetic parameters are listed in

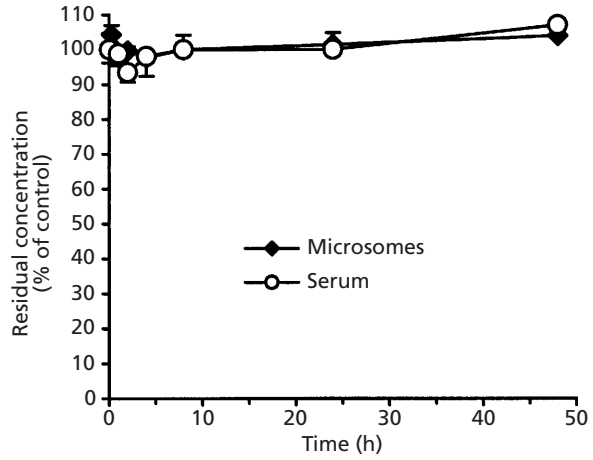

Figure 3 Stability of LJP 920 incubated with mouse serum and liver microsomes for varying times at 37°C. The percentage of LJP 920 remaining intact was calculated by integration of chromatographic peak area. No indication of degradation was found. Each point represents the mean ± s.d. of 3–4 tests.

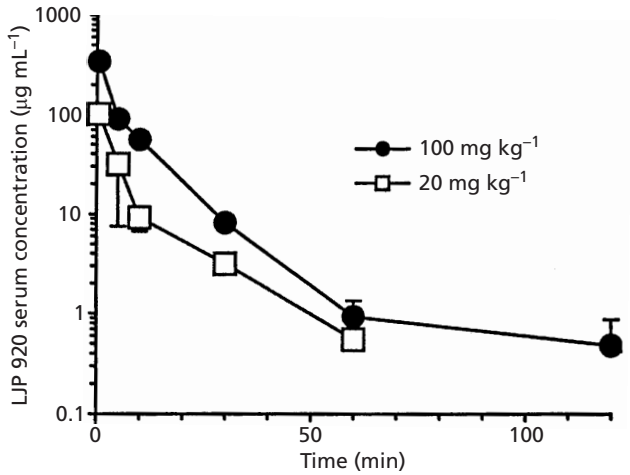

Figure 4 Serum concentration–time profiles of LJP 920 in mice after tail-vein injection of single doses (20 and 100 mg kg^{-1}). Each point represents the mean ± s.d. of three mice, each performed in duplicate.

Table 1 Serum pharmacokinetic parameters of intravenously administered LJP 920 in mice.

	Dose (mg kg^{-1})	
	20	100
$t_{\frac{1}{2}}\alpha$ (min)	2.44 ± 0.00	3.58 ± 0.13
$t_{\frac{1}{2}}\beta$ (min)	33.04 ± 0.01	42.18 ± 0.15
$t_{\frac{1}{2}k10}$ (min)	3.57 ± 0.00	2.45 ± 0.27
K_{10} (min^{-1})	0.19 ± 0.00	0.28 ± 0.03
K_{12} (min^{-1})	0.08 ± 0.00	0.12 ± 0.19
K_{21} (min^{-1})	0.03 ± 0.00	0.04 ± 0.05
C_{max} (μg mL^{-1})	116.47 ± 0.00	514.15 ± 48.59
CL (mL min^{-1})	0.67 ± 0.00	1.10 ± 0.02
AUC (μg min mL^{-1})	599.96 ± 0.05	1815.11 ± 29.73
V_{ss} (mL)	12.37 ± 0.01	9.76 ± 0.13

Values are means ± s.e. $t_{\frac{1}{2}}\alpha$, distribution half-life; $t_{\frac{1}{2}}\beta$, elimination half-life; $t_{\frac{1}{2}k10}$, half-life for drug leaving the system from the central compartment; K_{10}, rate constant at which the drug leaves the system from the central compartment; K_{12}, rate constant for the movement of drug from central to peripheral compartment; K_{21}, rate constant for the movement of drug from peripheral to central compartment; C_{max}, maximum serum concentration; CL, clearance; AUC, area under the curve; V_{ss}, volume of distribution at steady state.

Table 1. The C_{max} and AUC values of LJP 920 demonstrated dose proportionality in mice over the intravenous dose range of 20 and 100 mg kg^{-1}. The distribution half-life ($t_{\frac{1}{2}}\alpha$) was about 3 min, whereas the elimination half-life ($t_{\frac{1}{2}}\beta$) was 33 (20 mg kg^{-1}) and 42 min (100 mg kg^{-1}) for unchanged LJP 920 administered intravenously to mice (Table 1). The relative shortness of the half-lives was most likely due to the hydrophilic properties of carbohydrates and the poor affinity of carbohydrates for plasma protein binding, with dissociation constants in the millimolar range (Sears & Wong 1996), causing a quick disappearance of the drug from the mouse systemic circulation either by tissue distribution or renal excretion. Indeed, we found that the magnitude of the V_{ss} (volume of distribution at steady state) of LJP 920 (Table 1) was 10 times the mouse blood volume (approximately 4.5% body weight), suggesting that LJP 920 is more concentrated in extravascular tissues and less concentrated intravascularly. In addition, the high V_{ss} is indicative of low binding of the drug to plasma proteins.

The half-life of LJP 920, which is an octameric Gal (α1–3) Gal conjugate, measured in mice using the HPLC method is close to that reported by Nagasaka et al (1997), although a detailed pharmacokinetic analysis was lacking in their paper. Using radioactive labelling, Nagasaka et al showed that the half-lives of radiolabelled Gal (α1-3) Gal alone and its polyethylene glycol-conjugates in rats were about 18 min (5 mg per rat, i.v.) and 38 min (100 mg per rat, i.v.), respectively. The structural differences between their compounds and ours may cause variation in the hydrophilic characteristics of the conjugates, which consequently affect the elimination phase of the drug.

Tissue distribution and excretion

Tissue concentrations of LJP 920 were studied following a single intravenous dose of 100 mg kg^{-1}. The highest concentrations were found in the kidney and the lowest in the brain at 10 min after dosing (Table 2). The tissue levels of LJP 920 at 2 h after dosing fell to 0.5–5 μg g^{-1} in kidney, liver, lung, heart, spleen and muscle, and were under the detection limit in fat and brain.

Total removal or elimination of a drug from systemic circulation is affected by metabolism (biotransformation) and excretion. Since we have demonstrated that LJP 920 is stable in liver microsomes and plasma, the major elimination route of LJP 920 is likely via renal excretion. Indeed, the cumulative urinary recovery of unchanged LJP 920 within 4 and 8 h of dosing accounted for 12% and 23% of the total dose (100 mg, kg^{-1}), respectively. The cumulative faecal recovery of unchanged LJP 920 over 8 h was only 3% of the total dose. The fact that a greater proportion of LJP 920 was excreted as the unchanged drug strongly supports the proposal that enzymatic degradation is a minor route of elimination of LJP 920, whereas the renal excretion accounts for the major elimination of the drug. It will be

Table 2 Tissue levels (μg g^{-1}) of LJP 920 at 10 min after intravenous administration (100 mg kg^{-1}) to mice (n = 5).

Kidney	Liver	Lung	Heart	Spleen	Muscle	Fat	Brain
410 ± 98	280 ± 57	210 ± 41	157 ± 23	139 ± 16	42 ± 7	18 ± 1	13 ± 1

Values are means ± s.d.

of great interest to determine whether the tissue distribution may be another cause of the disappearance of LJP 920 from the systemic circulation. The assessment of in-vitro metabolism of LJP 920 at an early stage in its development excludes concerns regarding LJP 920's metabolic instability and will facilitate early rational planning of clinical studies.

An additional whole-blood sample for determination of the serum-to-erythrocyte concentration ratio was taken from each mouse at 0.5 and 5 min after LJP 920 administration (100 mg kg^{-1}, i.v.). A chromatographic analysis of LJP 920 in either serum or erythrocytes, respectively, following deproteinization and centrifugation showed that the serum-to-erythrocyte concentration ratio of LJP 920 was 33 and 36 at 0.5 and 5 min after injection. Erythrocyte concentrations of LJP 920 were substantially lower than serum concentrations, indicating that LJP 920 does not preferentially associate with erythrocytes and that the erythrocyte uptake accounts for only a negligible proportion of the total blood concentration of LJP 920. This finding raises the possibility that when LJP 920 is administered to xenograft recipients (i.e., Old World monkeys in preclinical studies and humans in clinical trials), most of the drug would beneficially concentrate and react in the sera where xenoreactive natural antibodies are predominantly present (Galili et al 1991; Sandrin et al 1993).

In conclusion, this study illustrates the in-vitro biostability of the octameric Gal (α1–3) Gal conjugate in liver microsomes and plasma. This conjugate is largely distributed in serum in comparison with blood cells. It quickly disappeared from the systemic circulation, and its elimination occurs mainly by renal clearance.

References

Birkett, D. J., Mackenzie, P. I., Veronese, M. E., Miners, J. O. (1993) In vitro approaches can predict human drug metabolism. *Trends Pharmacol. Sci.* **14**: 292–294

Bracy, L. J., Sachs, D. H., Iacomini, J. (1998) Inhibition of xenoreactive natural antibody production by retroviral gene therapy. *Science* **281**: 1845–1847

Gabrielsson, J., Weiner, D. (1996) *Pharmacokinetic and Pharmacodynamic Data Analysis: Concepts and Applications*, 2nd edn Swedish Pharmaceutical Press, Stockholm, Sweden

Galili, U. (1993) Interaction of the natural anti-gal antibody with α-galactosyl epitopes: a major obstacle for xenotransplantation in humans. *Immunol. Today* **14**: 480–482

Galili, U., Swanson, K. (1991) Gene sequences suggest inactivation of α-1,3-galactosyltransferase in catarrhines after the divergence of apes from monkeys. *Proc. Natl Acad. Sci. USA* **88**: 7401–7404

Galili, U., Clark, M. R., Shohet, S. B., Buehler, J., Macher, B. A. (1987) Evolutionary relationship between the natural anti-gal antibody and the gal α 1–3 gal epitope in primates. *Proc. Natl Acad. Sci. USA* **84**: 1369–1373

Galili, U., Anaraki, F., Thall, A., Hill-Black, C., Radic, M. (1993) One percent of human circulating B lymphocytes are capable of producing the natural anti-gal antibody. *Blood* **82**: 2485–2493

Jia, L., Young, X., Guo, W. (1999) Physicochemistry, pharmacokinetics, and pharmacodynamics of S-nitrosocaptopril crystals, a new nitric oxide donor. *J. Pharm. Sci.* **88**: 981–986

Joziasse, D. H., Shaper, J. H., Jabs, E. W., Shaper, N. L. (1991) Characterization of an α 1-3-galactosyltransferase homologue on human chromosome 12 that is organized as a processed pseudogene. *J. Biol. Chem.* **266**: 6991–6998

Larsen, R. D., Rivera-Marrero, C. A., Ernst, L. K., Cumming, R. D., Lowe, J. B. (1990) Frameshift and nonsense mutations in a human genomic sequence homologous to a murine UDP-Gal:β-D-Gal(1,4)-D-GlcNAc α(1–3)-galactosyltransferase cDNA. *J. Biol. Chem.* **265**: 7055–7061

Matsubara, T., Koike, M., Touchi, A., Tochino, Y., Sugeno, K. (1976) Quantitative determination of cytochrome P-450 in rat liver homogenate. *Anal. Biochem.* **75**: 596–603

Nagasaka, T., Kobayashi, T., Muramatsu, H., Fujimoto, H., Matsuo, I., Ajisaka, K., Kadomatsu, K., Hayashi, S., Yokoyama, I., Hayakawa, A., Muramatsu, T., Takagi, H. (1997) α-Galactosyl oligosaccharides conjugated with polyethylene glycol as potential inhibitors of hyperacute rejection upon xenotransplantation. *Biochem. Biophys. Res. Commun.* **232**: 731–736

Obach, R. S., Baxter, T. G., Liston, T. E., Silber, M. B., Jones, B. C., MaCintyre, F., Rance, D. J., Wastall, P. (1997) The prediction of human pharmacokinetic parameters from preclinical and in vitro metabolism data. *J. Pharmacol. Exp. Ther.* **283**: 46–58

Pearce, R. E., McIntyre, C. J., Madan, A., Sanzgiri,U., Draper, A. J., Bullock, P. L., Cook, D. C., Burton, L. A., Latham, J., Nevins, C., Parkinson, A. (1996) Effects of freezing, thawing, and storing human liver microsomes on cytochrome P450 activity. *Arch. Biochem. Biophys.* **331**: 145–169

Sandrin, M. S., Vaughan, H. A., Dabkowski, P. L., McKenzie, I. F. C. (1993) Anti-pig IgM antibodies in human serum react predominantly with gal(α1-3)gal epitopes. *Proc. Natl Acad. Sci. USA* **90**: 11391–11395

Sears, P., Wong, C. H. (1996) Intervention of carbohydrate recognition by proteins and nucleic acids. *Proc. Natl Acad. Sci. USA* **93**: 12086–12093

Yu, L., Xie, F., Jones, D. S., Ramirez, M. S., Jack, R. M. (1999) Development of multivalent toleragens to inhibit binding of human anti-galactose α 1,3 galactose antibodies. *Transplantation* **67**: S555